Three Dimensional Modeling of Enhanced Oil Recovery from Shale Reservoir

Nmegbu Chukwuma Godwin Jacob & Orisa Ebube Favour
Department of Petroleum Engineering,
Rivers State University of Science and Technology,
Port Harcourt, Nigeria.
gnmegbu@gmail.com, ebubeorisa@yahoo.com

Abstract
The development of shale reservoirs has proven to be difficult for the obvious reasons that they are tight reservoirs with very poor permeability, porosity and additionally, shale reservoirs have just been discovered recently and as such not many methods are available with regards to their development. In this project, published data from the Eagle Ford Shale was computed in a black-oil simulator ECLIPSE (E-300, Office 2015.1) which was used to simulate a number of production plans for gas flooding and water flooding. 8470 (22 x 55 x 7) grid-cells are used to build a 200ft long×1000ft wide×200ft thick reservoir model. Three typical production plans for gas and water injection were presented in this thesis respectively. Two half-vertical well with two 1-ft wide fractures where stimulated to represent two half-fractures. Miscible gas injection simulation results showed positive effect on improving shale oil recovery. Water injection in shale oil reservoir was not considered because of the inherent assumption that water injection has no potential in the development of shale oil reservoirs.

Keywords: *Eclipse, Modeling, Recovery, Shale, Fracturing.*

1. Introduction

The world energy demand has led to the discovery of unconventional reservoirs that were initially problematic to develop. Shale reservoir is an example of such reservoir systems. One of the main interests of the current petroleum industry is to explore methods that can economically produce from the previously unprofitable payzones such as shale reservoirs(Amy, 2015).In contemporary times, shale reservoirs have become a very important source of energy source (petroleum fluids), especially in countries such as US and Canada. The discovery of Shale oil has not only changed the slope depicted by production rates during the last few years from negative to positive making it a huge success but has led to outstanding creativity, innovation and resilience in the petroleum industry(Tao Wan, 2013). These results are significant as the endowment of oil, gas and condensate in shales throughout the world is quite gigantic. Not only has the development of shale reservoirs proven to be difficult for the obvious reasons that they are tight reservoirs wit very poor permeability but pressure distribution and flow modeling of unconventional fractured reservoirs (shale reservoirs) remains a big challenge for the petroleum industry. Shale is a sedimentary rock that contains kerogen that is released as petroleum-like liquids when the rock is heated in the chemical process of pyrolysis. Shale reservoirs are fine grained sediments with low porosity and extremely low permeability, which are both the source rock and the reservoirs (Javadpour, 2009). Although the study on the applicability and performance of enhanced oil recovery in shale reservoirs is a new phenomenon, several works has been done on the modeling and simulation of unconventional reservoir which has irregularities as well low matrix permeability. Fragoso *et al*, (2016) evaluated the possible use of continuous gas injection as well as huff and puff gas injection in the oil and condensate containers of the Eagle Ford shale.

They utilized single porosity, dual porosity and dual permeability numerical simulation for their purpose. In addition, they investigated the effect on recovery of bottom whole pressure (BHP), natural fracture permeability and spacing, hydraulic fracture length and spacing, and distance between parallel wells. They concluded that liquid recovery in shale condensate and shale oil reservoirs could be improved by means of dry gas injection.

Liu *et al*. (2014) simulated the EOR potential by CO_2 flooding using a sector model of Bakken formation in the Bailey and Grenora areas of the Western North Dakota. The modeled area includes a pair of existing horizontal wells with a spacing of 3000 ft. These two wells are known to be in communication. Their results show that CO_2 flooding can enhance oil production (recovery) by 43% when fracture relative permeability curves are used, or 58% when matrix relative permeability curves are used, compared to their respective cases without CO_2 flooding. Those increased oil production percentages correspond to the net CO_2 utilization values of 5.86 and 23.175 MSCF/STB, respectively. Their results indicate that the relative permeability curves used in the model are very sensitive. Hoteit, (2011) focused his study on the proper modeling of diffusion flux, determination of the diffusion coefficient, and the mass transfer at the fracture-matrix interface during CO_2 EOR processes in naturally fractured reservoirs. Hoteit, (2011) stated in his work that the proper modeling of diffusion mechanisms is often neglected during reservoir engineering due to the facts that convection is the predominate fluid transport mechanism in most conventional recovery processes, and the artificial dispersion calculated by numerical methods is often high enough to compensate for diffusion. This finding was in accordance with the work of (McKay 1971; Darvish*et al*. 2006). However, he concluded that molecular diffusion in the cases of heavy oil recovery and gas injection in fractured reservoirs with low matrix permeability is the dominate mechanism for oil production, and cannot be excluded during the modeling process. He also emphasized on the importance of modeling cross phase diffusion at the CO_2-oil interface. Vega *et al.* (2010) simulated their miscible experiments with CMG GEM single porosity model. Their investigation mainly focused on the effect of core heterogeneity and diffusion, and drew the following conclusions. The co-current model (forced injection) was sensitive to the presence of high/low permeability channels, whereas in the countercurrent model, production was not significantly affected by permeability heterogeneity. Wan and Sheng (2015) used the CMG dual permeability model coupled with diffusion equations for their reservoir simulation of gas flooding. They concluded the dual permeability model is more time efficient and can capture the matrix-fracture mass transfer properly. In addition, from their field scale simulation results, they drew the conclusion that the dominate recovery mechanism in low permeability shale reservoirs is diffusion, and the effect of diffusion on recovery is significant. Chen *et al.* (2014) used an EOS based compositional simulator UT-COMP to simulate the effect of heterogeneity on primary recovery as well as the CO_2 huff n puff process in the Bakken. In their study, CO_2 dispersion is resulted from first contact or multiple contact miscibility during injection. They concluded CO_2 migration into the shale matrix is very limited due to the low matrix permeability. The study conducted by Gamadi *et al.* (2014) evaluated the potential of natural gas injection in the Eagle Ford Shale. They concluded that the soaking period has significant effect on the ultimate recovery. The study conducted by Rivera (2014) took diffusion into consideration in his study. However, since his model was built with the CMG GEM single porosity model, the cross phase diffusion is neglected in his simulation. The higher recovery resulted from inter phase diffusion is purely due to the initial convection caused by pressure gradient. Example of similar other studies include Holme (2013), Wan *et al*. (2013), Liu *et al*. (2014). Shuler *et al*. (2016) have described a conventional surfactant ‘huff-n-puff' treatment to investigate the relationship between increased oil production and the surfactant soaking period.

Surfactant chemistry is considered as a possible IOR solution. The authors indicated that if properly selected and designed, the surfactant additives in stimulation/fracturing fluids could have multi-functions towards improving both IP and the longer-term oil production. Shuler *et al*. (2016) have described a conventional surfactant 'huff-n-puff' treatment to investigate the relationship between increased oil production and the surfactant soaking period. Surfactant chemistry is considered as a possible IOR solution. The authors indicated that if properly selected and designed, the surfactant additives in stimulation/fracturing fluids could have multi-functions towards improving both IP and the longer-term oil production. Wang *et al*. (2016a) investigated the use of surfactant imbibition to increase oil recovery in shales. They used cores from the Bakken Formation in North Dakota saturated with crude oil from the same formation. A number of surfactant formulations and brine were used for imbibition studies. They concluded that if the shale can be properly contacted by the surfactant, oil recovery can be significantly increased. Experimental work conducted by Tovar *et al*. (2014) used supercritical CO_2 and preserved sidewall shale cores. A similar study with both static (soaking) and dynamic (direct injection) CO_2 conducted by Hawthorne *et al*. (2013) using Bakken cores with low and ultra-low permeability showed that CO_2 is capable of producing a significant percentage of the oil inside tight shale cores with enough exposing times.

2. Model Formulations

The model to be developed will be based on these production features in shale reservoir systems. The components and assumptions of the model are:

- **i.** Low reservoir permeability
- **ii.** Water flooding operation active
- **iii.** Gas flooding operation active
- **iv.** Presence of inclined fractures
- **v.** Uniform size and length of fractures
- **vi.** Constant gas and water injection
- **vii.** Isothermal reservoir
- **viii.** No flow across the boundaries of the reservoir

Considering a rectangular shale reservoir control volume with dimensions Δx , Δy and Δz , containing horizontal fractures as shown in figure 2.1.

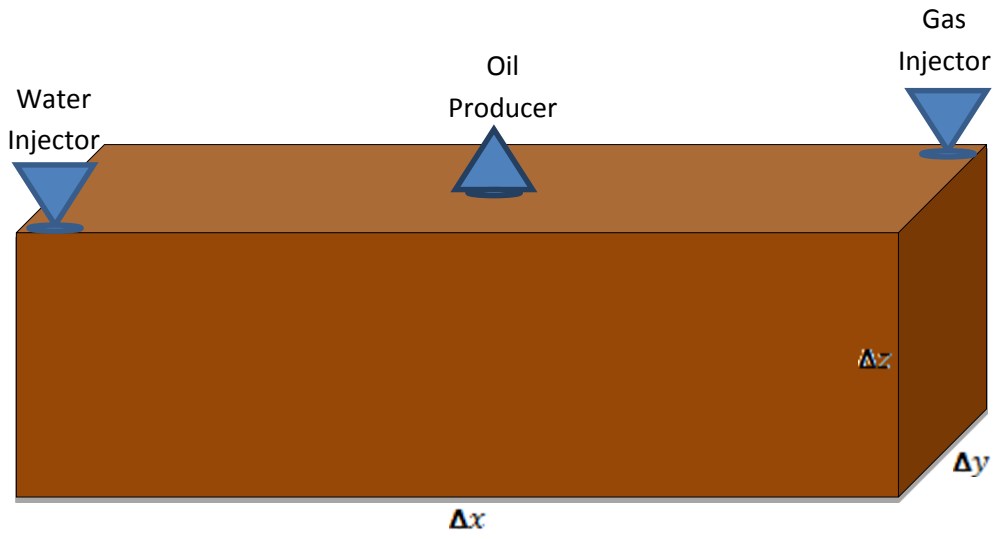

Figure 2.1: A pictorial representative of the shale reservoir model.

If the mass flux inflow through the x-direction is $\rho\alpha_x$ and the mass outflow is $\rho\alpha_x + \Delta(\rho\alpha_x)$, and if the mass flux inflow through the y-direction is $\rho\alpha_y$ and the mass outflow is $\rho\alpha_y + \Delta(\rho\alpha_y)$ and that of the z direction is given as $\rho\alpha_z$ and $\rho\alpha_z + \Delta(\rho\alpha_z)$, the mass balance of the system can be written as:

$$Mass\ rate\ in - Mass\ rate\ Out + Injected\ mass\ rate = acccumulation\ rate \quad (3.2)$$

$$Total\ mass\ rate\ in = \rho\alpha_x\Delta y\Delta z + \rho\alpha_y\Delta x\Delta z + \rho\alpha_z\Delta x\Delta y \quad (3.3)$$

$$Total\ mass\ rate\ out = [\rho\alpha_x + \Delta(\rho\alpha_x)]\Delta y\Delta z + [\rho\alpha_y + \Delta(\rho\alpha_y)]\Delta x\Delta z + [\rho\alpha_z + \Delta(\rho\alpha_z)]\Delta x\Delta y \quad (3.4)$$

The net injected rate is given as $q_{tn} = q_{wi} + q_{gi}$

The Accumulation in this fracture study will be a function of the porosity variation with time as well fracture volume variation with pressure change. The total accumulation is given as:

$$Accumulation = Accumulation\ in\ pores + Accumulation\ in\ fractures$$

Therefore,

$$Accumulation = \left(\frac{\rho\emptyset_{t+\Delta t} - \rho\emptyset_t}{\Delta t}\right)(\Delta x\Delta z\Delta y - V_{f(t)}) + \frac{\rho V_{f(t+\Delta t)} - \rho V_{f(t)}}{\Delta t} \quad (3.5)$$

Substituting all these parameters into equation 3.2 and simplifying we have it that:

$$-\Delta(\rho\alpha_x)\Delta y\Delta z - \Delta(\rho\alpha_y)\Delta x\Delta z - \Delta(\rho\alpha_z)\Delta x\Delta y = \left(\frac{\rho\emptyset_{t+\Delta t} - \rho\emptyset_t}{\Delta t}\right)(\Delta x\Delta z\Delta y - V_{f(t)}) + \frac{\rho V_{f(t+\Delta t)} - \rho V_{f(t)}}{\Delta t} \quad (3.6)$$

Dividing both sides by the bulk volume $\mathbf{V_B} = \Delta x\Delta z\Delta y$, we have that:

$$-\frac{\Delta(\rho\alpha_x)}{\Delta x} - \frac{\Delta(\rho\alpha_y)}{\Delta y} - \frac{\Delta(\rho\alpha_z)}{\Delta z} + \frac{q_{win}}{\mathbf{V_B}} = \left(\frac{\rho\emptyset_{t+\Delta t} - \rho\emptyset_t}{\Delta t}\right)\left(1 - \frac{V_f}{\mathbf{V_B}}\right) + \frac{1}{\mathbf{V_B}}\frac{\rho V_{f(t+\Delta t)} - \rho V_{f(t)}}{\Delta t} \quad (3.7)$$

As $\Delta x, \Delta z, \Delta y\ and\ \Delta t \to 0$ $then\ \Delta \to \partial$, $therefore\ equation\ 3.7\ becomes$:

$$-\frac{\partial}{\partial x}(\rho\alpha_x) - \frac{\partial}{\partial y}(\rho\alpha_y) - \frac{\partial}{\partial z}(\rho\alpha_z) + \frac{q_{win}}{\mathbf{V_B}} = \frac{\partial}{\partial t}(\rho\emptyset)\left(1 - \frac{V_f}{\mathbf{V_B}}\right) + \frac{1}{\mathbf{V_B}}\frac{\partial}{\partial t}(\rho V_f) \quad (3.8)$$

Equation 3.8 is the general mass balance (or continuity equation), where ρ is the density of the fluid, α is the volume flux, V_f is the volume of the fracture, $\mathbf{V_B}$ is the bulk volume, and $\emptyset$ is the porosity of the system.

A modification of the Darcy's model for volume flux (or velocity) including velocity in the inclined fracture is given as:

$$\alpha_x = -\beta\left(\frac{k_x}{\mu}\frac{\partial P}{\partial x} + \frac{k_f}{\mu}\rho sin\theta\right) \quad (3.9)$$

$$\alpha_y = -\beta\left(\frac{k_y}{\mu}\frac{\partial P}{\partial y} + \frac{k_f}{\mu}\rho cos\theta\right) \quad (3.10)$$

For the z–direction, we neglected gravitational effect; therefore fracture contribution to the volume flux in the z direction is equal to zero. In that case

$$\alpha_z = -\beta\left(\frac{k_z}{\mu}\frac{\partial P}{\partial z}\right) \quad (3.11)$$

The relationship between formation volume factor and density is given as:

$$B = \frac{\rho_{sc}}{\rho} \quad (3.12)$$

Therefore,

$$\rho = \frac{\rho_{sc}}{B} \quad (3.13)$$

The mass flowrate in equation 3.8 can be converted to volume rate as:

$$Q_{tn} = \frac{q_{tn}}{\rho_{sc}} \quad (3.14)$$

That is:

$$Q_{tn} = q_{tn}\,\rho_{sc}$$

Substituting these expressions into equation 3.8 we have that:

$$\frac{\partial}{\partial x}\left[\frac{\rho_{sc}}{B}\beta\left(\frac{k_x}{\mu}\frac{\partial P}{\partial x}\right)\right]+\frac{\partial}{\partial y}\left[\frac{\rho_{sc}}{B}\beta\left(\frac{k_y}{\mu}\frac{\partial P}{\partial y}\right)\right]+\frac{\partial}{\partial z}\left(\frac{\rho_{sc}}{B}\beta\left(\frac{k_z}{\mu}\frac{\partial P}{\partial z}\right)\right)+\frac{Q_{tn}\,\rho_{sc}}{\mathbf{V_B}}=\frac{\partial}{\partial t}\left(\frac{\rho_{sc}}{B}\emptyset\right)\left(1-\frac{V_f}{\mathbf{V_B}}\right)+\frac{1}{\mathbf{V_B}}\frac{\partial}{\partial t}\left(\frac{\rho_{sc}}{B}V_f\right) \quad (3.15)$$

Eliminating constants on both sides and simplifying, the equation becomes:

$$\frac{\partial}{\partial x}\left(\frac{k_x}{B\mu}\frac{\partial P}{\partial x}\right)+\frac{\partial}{\partial y}\left(\frac{k_y}{B\mu}\frac{\partial P}{\partial y}\right)+\frac{\partial}{\partial z}\left(\frac{k_z}{B\mu}\frac{\partial P}{\partial z}\right)+\frac{Q_{tn}}{\beta\mathbf{V_B}}=\frac{1}{\beta}\frac{\partial}{\partial t}\left(\emptyset\frac{}{B}\right)\left(1-\frac{V_f}{\mathbf{V_B}}\right)+\frac{1}{\beta\mathbf{V_B}}\frac{\partial}{\partial t}\left(\frac{V_f}{B}\right) \quad (3.16)$$

Equation 3.16 is for unit reservoir volume. Multiplying equation 3.16 by the reservoir volume

$$V_B = A_x\Delta x = A_y\Delta y = A_z\Delta z \quad (3.17)$$

Equation 3.16 becomes:

$$\frac{\partial}{\partial x}\left(\frac{k_xA_x}{B\mu}\frac{\partial P}{\partial x}\right)\Delta x+\frac{\partial}{\partial y}\left(\frac{k_yA_y}{B\mu}\frac{\partial P}{\partial y}\right)\Delta y+\frac{\partial}{\partial z}\left(\frac{k_zA_z}{B\mu}\frac{\partial P}{\partial z}\right)\Delta z=\frac{1}{\beta}\frac{\partial}{\partial t}\left(\emptyset\frac{}{B}\right)(\mathbf{V_B}-V_f)+\frac{1}{\beta}\frac{\partial}{\partial t}\left(\frac{V_f}{B}\right)-\frac{q_{tn}}{\beta} \quad (3.18)$$

In equation 3.18, the permeability term is an average of the matrix permeability and the fracture permeability. The shale average permeability can be derived from the model representing the geometric permeability average for heterogeneous unconventional reservoirs described in Jones & Roland, 2018 as:

$$k_{xavg} = e^{\left[\frac{V_B}{V_f}\ln\left(\frac{k_{xm}\times k_f}{k_{xm}+k_f}\right)\right]} \quad (3.19)$$

Similarly, in the y and z directions we have that:

$$k_{yavg} = e^{\left[\frac{V_B}{V_f}\ln\left(\frac{k_{ym}\times k_f}{k_{ym}+k_f}\right)\right]} \quad (3.20)$$

$$k_{zavg} = e^{\left[\frac{V_B}{V_f}\ln\left(\frac{k_{zm}\times k_f}{k_{zm}+k_f}\right)\right]} \quad (3.21)$$

Equation 3.18 becomes:

$$\frac{\partial}{\partial x}\left(\frac{k_{xavg}A_x}{B\mu}\frac{\partial P}{\partial x}\right)\Delta x+\frac{\partial}{\partial y}\left(\frac{k_{yavg}A_y}{B\mu}\frac{\partial P}{\partial y}\right)\Delta y+\frac{\partial}{\partial z}\left(\frac{k_{zavg}A_z}{B\mu}\frac{\partial P}{\partial z}\right)\Delta z=\frac{1}{\beta}\frac{\partial}{\partial t}\left(\emptyset\frac{}{B}\right)(\mathbf{V_B}-V_f)+\frac{1}{\beta}\frac{\partial}{\partial t}\left(\frac{V_f}{B}\right)-\frac{q_{tn}}{\beta}$$

This is a flow and compositional model for a shale reservoir with fractures. The model accounts for the matrix permeability of the reservoir (which is usually very small) and the fracture permeability accounting for natural and artificial fractures. The model is a single phase oil flow model in a horizontal shale reservoir with natural and artificial fractures. Discretization of this equation is possible using the method finite difference approximation. After discretization the pressure distribution in the reservoir will be simulated for when the reservoir is composed of fractures and for when it is not.

2.1 Model Discretization

Re-writing equation 3.18 for a one dimensional reservoir consideration and substituting the expression.

$$B = \frac{B_o^i}{[1+c(p-p_i)]} \quad (3.23)$$

into the right hand side of the equation we have that:

$$\frac{1}{\Delta x_i}\left[\left(\frac{\beta_c k_{xavg}A_x}{B\mu}\frac{\partial P}{\partial x}\right)_{i+\frac{1}{2}}-\left(\frac{\beta_c k_{xavg}A_x}{B\mu}\frac{\partial P}{\partial x}\right)_{i-\frac{1}{2}}\right]\Delta x=\left(\frac{\mathbf{V_B}\emptyset c_t}{\alpha_c B}\frac{\partial P}{\partial t}\right)(\mathbf{V_B}-V_f)+\frac{\partial}{\partial t}\left(\frac{\mathbf{V_B}V_f c_t}{\alpha_c B}\frac{\partial P}{\partial t}\right)-q_{winsc}$$

Simplifying the expression we have that:

$$\left[\left(\frac{\beta_c k_{xavg}A_x}{B\mu}\frac{\partial P}{\partial x}\right)_{i+\frac{1}{2}}-\left(\frac{\beta_c k_{xavg}A_x}{B\mu}\frac{\partial P}{\partial x}\right)_{i-\frac{1}{2}}\right]=(\mathbf{V_B}-V_f)\left(\frac{\mathbf{V_B}\emptyset c_t}{\alpha_c B}\right)\left(\frac{\partial P}{\partial t}\right)_i+\left(\frac{\mathbf{V_B}V_f c_t}{\alpha_c B}\right)\left(\frac{\partial^2 P}{\partial t^2}\right)_i-q_{winsc}$$

Separating the pressure differential terms we have that:

$$\left[\left(\frac{\beta_c k_{xavg}A_x}{B\mu}\right)_{i+\frac{1}{2}}\left(\frac{\partial P}{\partial x}\right)_{i+\frac{1}{2}}-\left(\frac{\beta_c k_{xavg}A_x}{B\mu}\right)_{i-\frac{1}{2}}\left(\frac{\partial P}{\partial x}\right)_{i-\frac{1}{2}}\right]+\left(\frac{\mathbf{V_B}\emptyset c_t}{\alpha_c B}\right)\left(\frac{\partial P}{\partial t}\right)_i+\left(\frac{\mathbf{V_B}V_f c_t}{\alpha_c B}\right)\left(\frac{\partial^2 P}{\partial t^2}\right)_i-q_{winsc}$$

$$\left(\frac{\partial P}{\partial x}\right)_{i+\frac{1}{2}} = \frac{P_{i+1} - P_i}{\Delta x} \quad (3.26)$$

$$\left(\frac{\partial P}{\partial x}\right)_{i-\frac{1}{2}} = \frac{P_i - P_{i-1}}{\Delta x} \quad (3.27)$$

$$\left(\frac{\partial P}{\partial t}\right)_i = \frac{P_i^{n+1} - P_i^n}{\Delta t} \quad (3.28)$$

$$\left(\frac{\partial^2 P}{\partial t^2}\right) = \frac{P_i^{n+1} - P_i^n}{2\Delta t} \quad (3.29)$$

Substituting the expressions for the pressure differentials, the equation becomes:

$P_i^{n+1} - P_i^{\uparrow}$

Simplifying the expression we have that:

$P_{\downarrow}i^{\uparrow}n+1/[(V_{\downarrow}B-V_{\downarrow}f)((V_{\downarrow}B\emptyset c_{\downarrow}t)/(\Delta t\alpha_{\downarrow}c\,B))+((V_{\downarrow}B\,V_{\downarrow}f\,c_{\downarrow}t)/(\alpha_{\downarrow}c\,B\Delta t))\,]\,[((\llbracket\beta_{\downarrow}c\,k\rrbracket_{\downarrow}xavg\,A_{\downarrow}x)/B\mu\Delta x)_{\downarrow}(i+1/2)\,\llbracket P^{\uparrow}n\rrbracket_{\downarrow}(i+1)-[((\llbracket\beta_{\downarrow}c\,k\rrbracket_{\downarrow}xc$ (3.3

Equation 3.30 is modified for three dimension and is solved algebraically to obtain the behavior of pressure in the reservoir system during waterflooding.

3. Results and Discussion

The Eagle Ford shale is one of the most recent developments in unconventional exploration that trends across Texas from the Mexican Border in the South into East Texas, roughly 50 miles wide and 400 miles long. It is located in several counties stretching Giddings field in Brazos and Grimes counties down into the Maverick Basin in Maverick County. For this model, hydraulic fracture will be imposed in the eagle ford shale described in the previous section in other reproduce a real case scenario of shale reservoir development.

Table 4.2 Properties of the Design Hydraulic Fractures.

Properties	Value
Fracture Stages	10
Fracture Spacing	200 ft
Fracture Conductivity	83.3 md-ft
Fracture Half-length	500 ft
Fracture Cell Width	2 ft

Table 4.3: Relative Permeability End Point Values for Fracture and Matrix

Parameter	**Matrix**	**Fracture**
N_o	5	1.5
N_g	2	1
Interstitial water saturation S_{wi}	0.3	0.05
Residual gas saturation, S_{org}	0.3	0.1
Critical Gas Saturation, S_{gc}	0.05	0
K_{rg} at S_{org}	1	1

Modeling the whole Eagle ford reservoir may contain tremendous number of grid blocks, and it is of course time-consuming to model these complex fracture networks. Thus, we built a small shale oil reservoir model which is 250ft long×1200ft wide×20 ft thick. We develop this small part of shale oil reservoir with two vertical wells with single fracture respectively. The reservoir properties data used in this model is also from published data in Eagle Ford shale (Bazan, Larkin, et al. 2010). As shown in Fig 4.3, 8960 (20 x 56 x 8) grid-cells are used to simulate this part of reservoir. In this model we use 1-ft wide cells with 41.65 md-ft

conductivity which was located at the boundary of reservoir model to simulate the physical flow between two hydraulic fractures.

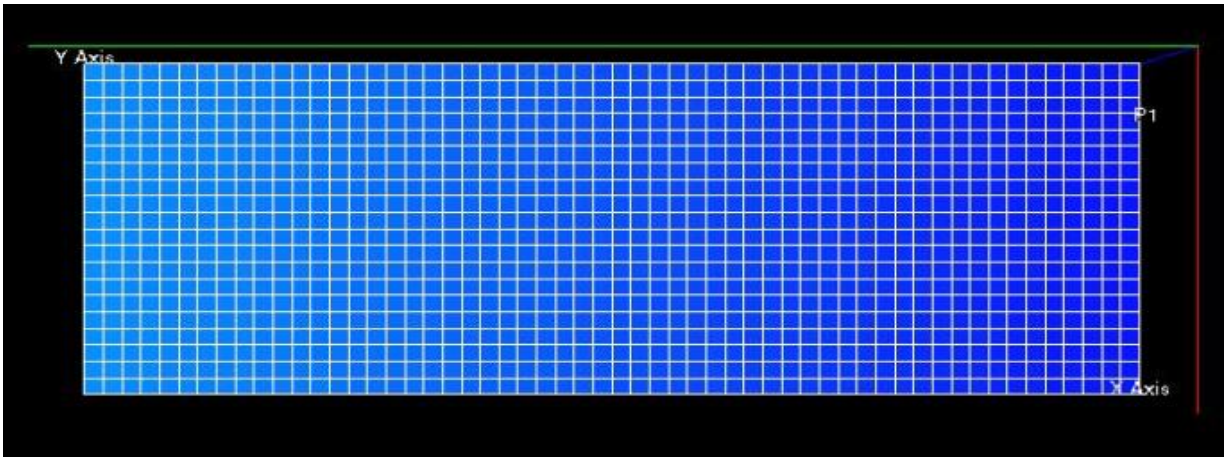

Figure 4.1: Reservoir Model Used For Simulation Analysis

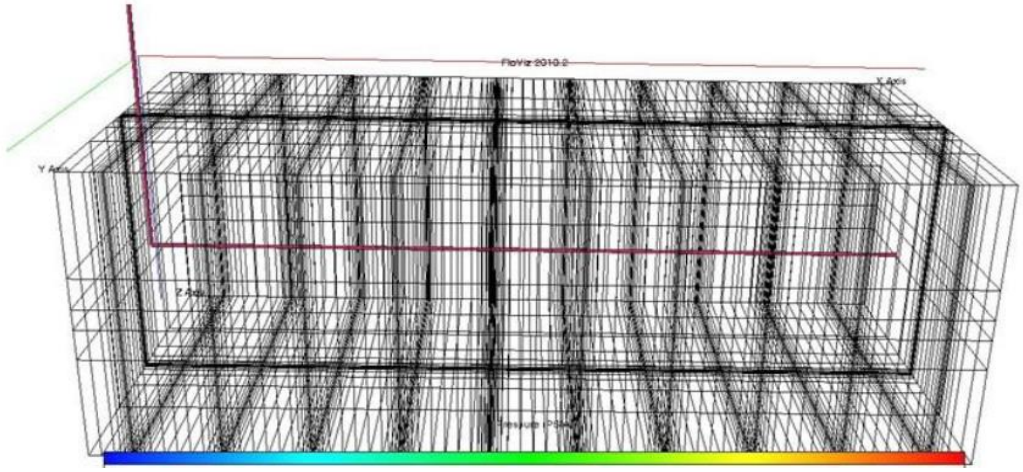

Figure 4.2: Model with a Single Horizontal Well

Two cases were considered to determine the effect of hydraulic fractures. Two models were used to test the results from the model with a 2-ft hydraulic fracture and the model which has two 1-ft hydraulic fractures.

Case 1
7200days of Primary production (200ft long×1000ft wide×200 ft thick, one 2-ft wide fracture)

Case 2
7200 days of Primary production (200ft long×1000ft wide×200 ft thick, two 1-ft wide fractures)
The purpose of this analysis is to determine the impact of fracture configuration on recovery potential of shale reservoirs. Both cases contain the same over size of fractures; but while one contains a single volume of fracture, the other one has the total volume split into two equal fracture volumes.

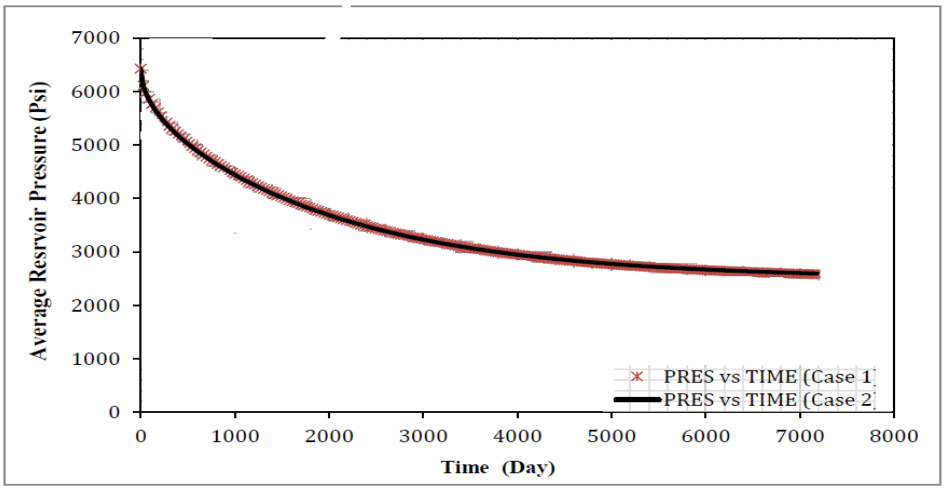

Figure 4.3 Reservoir Average Pressure vs Time

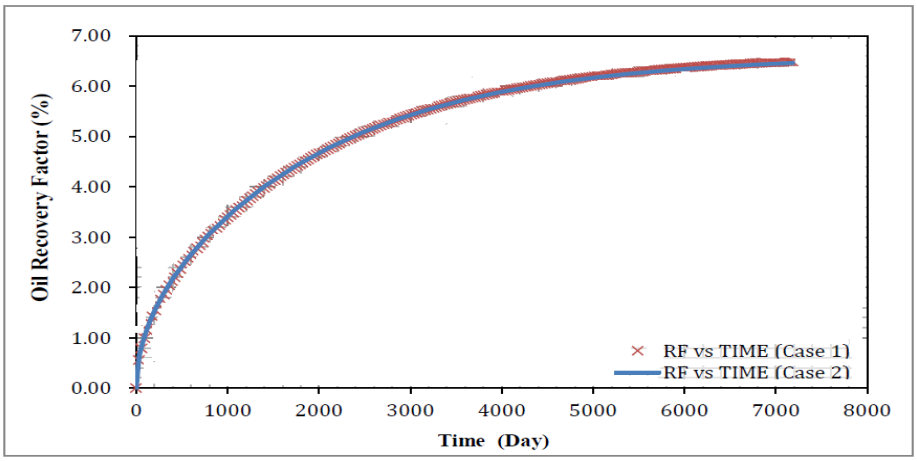

Figure 4.4 Field Oil Recovery Factor vs Time

As shown in Fig 4.3 and Fig 4.4, the average shale reservoir pressure depletion curve and oil recovery factor curve for two models matches perfectly for every time step. The cumulative oil production for case 1 is 16.456 MSTB and it is 16.533 MSTB in case 2. This indicates that configuration notwithstanding, a particular volume of hydraulic fracture, irrespective of how they are split through the entire reservoir system would cause the same recovery potentiality.

Table 4.4: Showing Validation of Models of Oil in Two Cases

	Case 1	Case 2
Cumulative Oil Production (MSTB)	16.456	16.533
Current Fluids In Place (MSTB)	234.95	235.15
Overall Recovery (%)	6.55	6.59

Gas Injection

To further the analysis performed in the previous section, gas injection was simulated for the model. To understand the actual effect of the gas injection process, the simulation was performed first without gas injection for 7200 days, then with gas injection and consequent production.

Case 3
7200 days of Primary production+30 cycles of gas injection, each cycle includes: 200 days injection and 200 days production (200ft long×1000ft wide×200 ft thick, one 2-ft wide fracture).

Case 4
7200 days of Primary production+30 cycles of gas injection, each cycle includes: 200 days injection and 200 days production (200ft long×1000ft wide×200 ft thick, two 1-ft wide fractures)
In this analysis we select a production scenario which has 7200-day primary production followed with 30 cycles of miscible gas injection, each cycle includes 200days injection and 200 days production and the well is also controlled by bottom hole pressure (BHP) which is set up as 2500 psi (Case 3: For one 2-ft wide fracture; Case 4: Two 1-ft wide fractures).

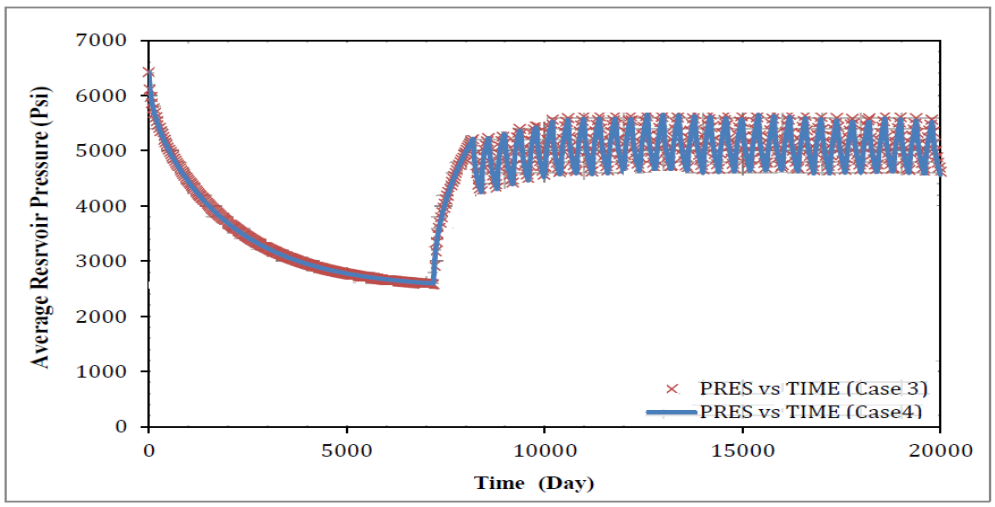

Figure 4.5 Reservoir Average Pressure vs Time

Fig 4.5 shows that the average reservoir pressure change of two models are consistent with each other, after 7200 days of primary production, a 1000-day gas injection was implemented to increase the reservoir pressure from 2450 psi to 5000psi and then 30 cycles of gas injection were applied. In cyclic injection period, the average reservoir pressure variations almost follow the same magnitude of fluctuation for each cycle.

Table 4.4: Showing Validation of Gas Injection in Two Cases

	Case 3	Case 4
Cumulative Oil Production (MSTB)	64.233	63.994
Current Fluids In Place (MSTB)	187.45	235.15
Overall Recovery (%)	25.37	24.88

From Fig 4.6 we can figure out that these two models have the same tendency of enhancing oil recovery effect. In the first 7200-day primary production period, the oil recovery factor is about 6.5% and then from the beginning of the cyclic gas injection, cumulative oil production has been increasing, finally, about 25 % oil recovery factor is achieved. The cumulative oil production for case 3 is 63.979 MSTB while it is 62.316 MSTB in case 4 (Table 4.5). After applying two production scenarios on two models, simulation results from our basic model are almost the same with Tao Wan's model. Thus, it's accurate to use our basic model to evaluate the potential of gas and water injection in shale oil reservoir.

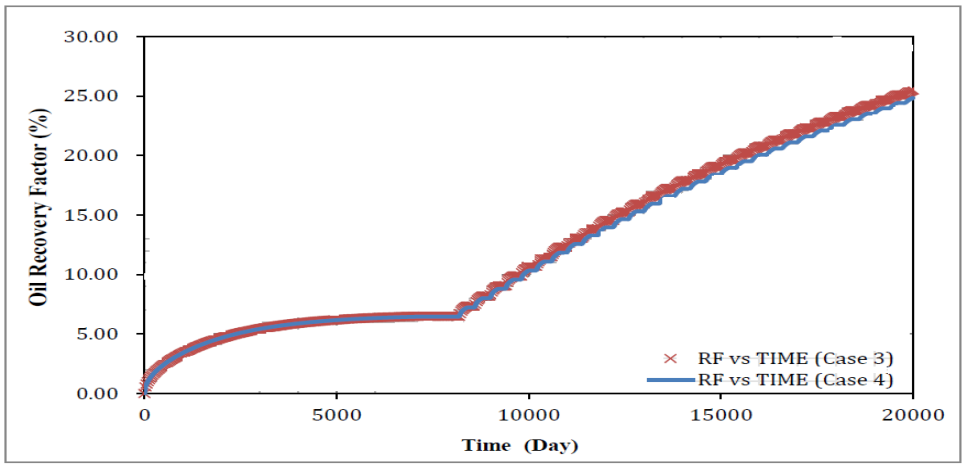

Figure 4.6 Field Oil Recovery Factor vs Time

The production behavior and recovery of oil from the low permeability shale formation is a function of the rock, fluid and the fracturing operations. Sensitivity analysis is a quantitative method of determining the important parameters which affect shale oil production performance. The parameters considered in this thesis include fracture half-length, flowing bottom-hole pressure, rock compressibility and matrix permeability. Sensitivity studies are necessarily for designing better simulation model and understanding the fundamental behavior of shale oil production system.

The fracture half-length used in the base model is 500 ft. Three another fracture half-lengths of 365 ft, 245 ft, 125 ft are selected to compare the effect of fracture length on shale oil production. Figure 4.7, 4.8 and 4.9 show the results of the different fracture half-length on the average reservoir pressure, cumulative oil production, oil rate, and recovery factor. The graph of average reservoir pressure for different fracture half-length shows that, the reservoir pressure decreases faster in case of longer fracture half-length. The average reservoir pressure at the end of 20 years for 500 ft fracture half-length is close to the bottom hole pressure limit of 2500 psi. The reservoir average pressure stays higher with shorter fracture half-length, leading lower ultimate oil recovery factor.
Longer fracture length means higher drainage volume of reservoir and hence the well can achieve higher initial production rate which will lead a higher cumulative oil production and higher ultimate recovery factor.

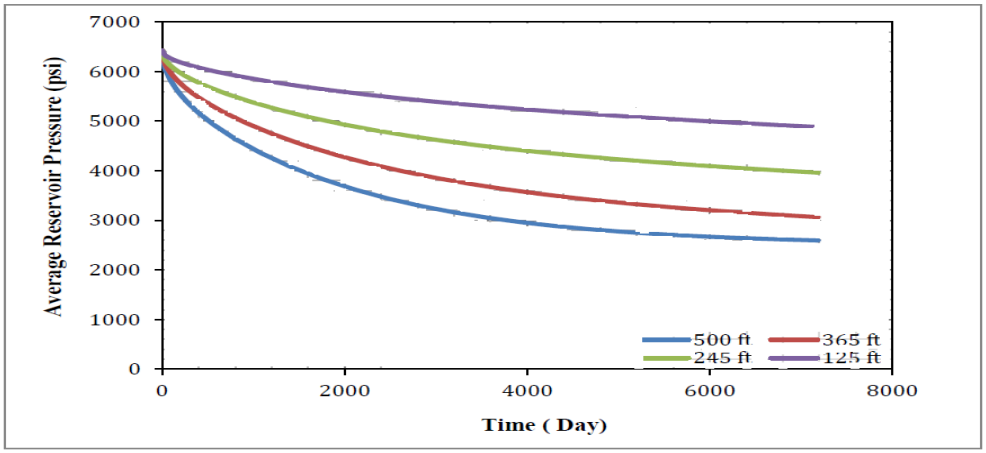

Figure 4.7 Reservoir Average Pressure vs Time (Fracture Half-length Sensitivity)

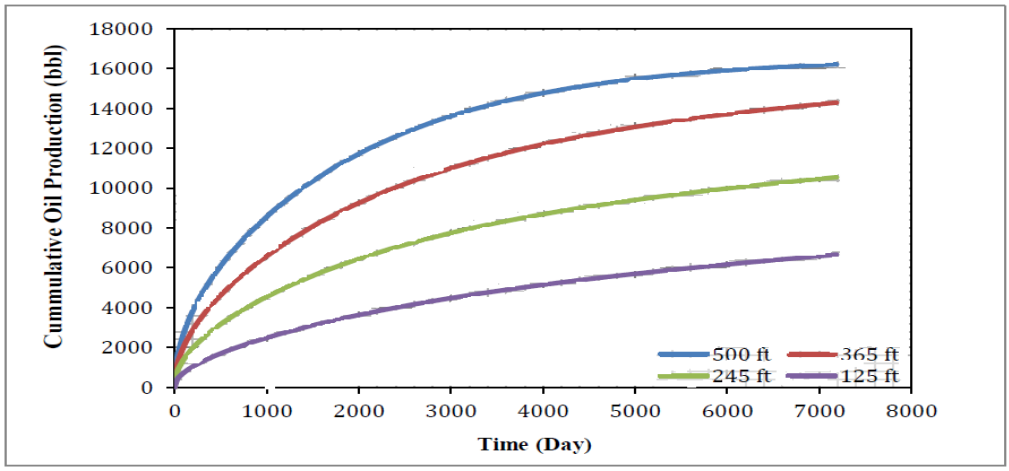

Figure 4.8 Cumulative Oil Production vs Time (Fracture Half-length Sensitivity)

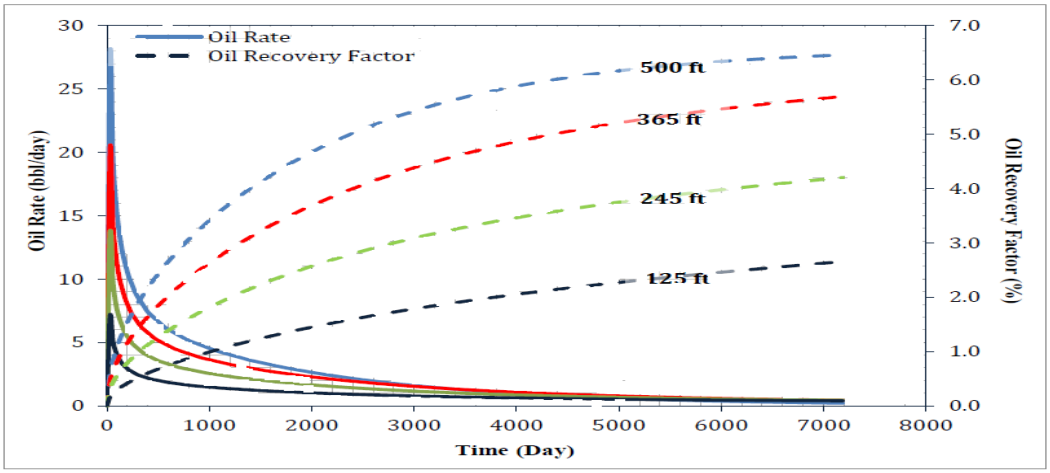

Figure 4.9 Oil rate and oil recovery factor vs. time (Fracture Half-length Sensitivity)

Figs 4.10 - 4.12 show the results for different matrix permeability, k values on the cumulative oil production, recovery factor, average reservoir pressure, and oil rate. The permeability value used in the base model is 0.0001 md (100 nano-darcy). Another three permeability values of 0.001 md, 0.0005 md and 0.00005 md are selected in matrix permeability sensitivity analysis. Because base model is controlled by bottom hole pressure which is set to 2500 psi, the average reservoir pressure for these four cases cannot be lower than 2500psi. Although the reservoir pressure is controlled to 2500 psi and the final oil recovery factor stays close for all cases, the advantage of higher matrix permeability can be pointed out easily. In case of 0.00005md, after 20 years production, the average pressure was not lowered much. But with higher matrix permeability, the reservoir pressure can decline rapidly to the 2500 psi limit set for the flowing bottom-hole pressure as showed in 0.001 md and 0.0005 md case. The cumulative oil production and oil recovery factor results show that at the end of 20 years production, 6.5% and 5.7% oil recovery can be obtained from 0.0001 md and 0.00005 md cases respectively. But for higher matrix permeability cases such as 0.001 md and 0.0005 md, to get the same oil recovery, only two and four years are needed. Higher matrix permeability means better hydraulic conductivity, leading higher initial oil rate and higher cumulative oil production.

The recovery from the formation with various permeabilities can be distinctly different. Shale permeability can be quite difficult to quantify. Core measurements are typically orders of magnitude lower than the effective shale permeability, but a conventional formation test or

buildup test is not possible with such low permeability. Mohamed, et al (2011) showed that analysis of fracture calibration tests may provide shale permeability, particularly if the test uses a very low injected volume.

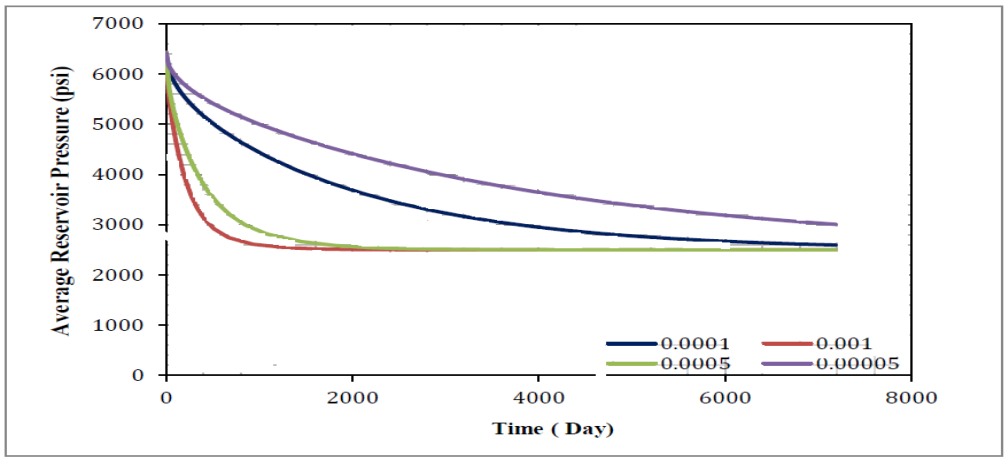

Figure 4.10 Reservoir Average Pressure vs Time (Matrix Permeability Sensitivity)

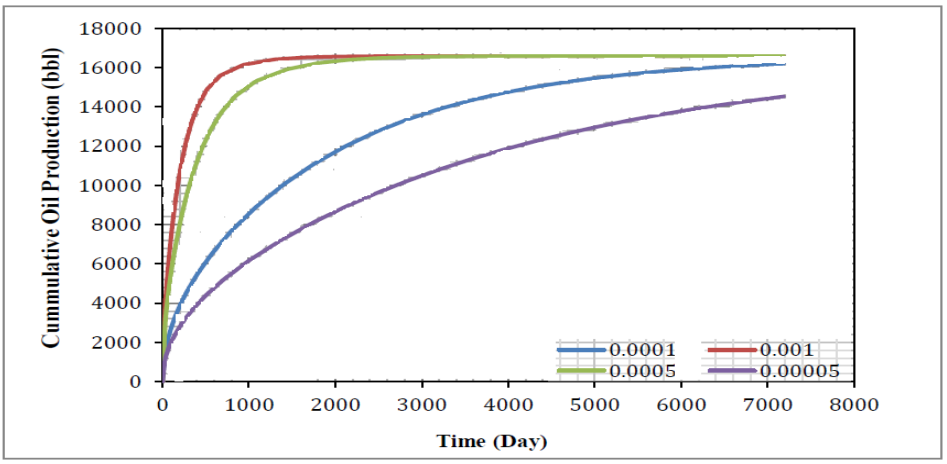

Figure 4.11 Cumulative Oil Production vs Time (Matrix Permeability Sensitivity)

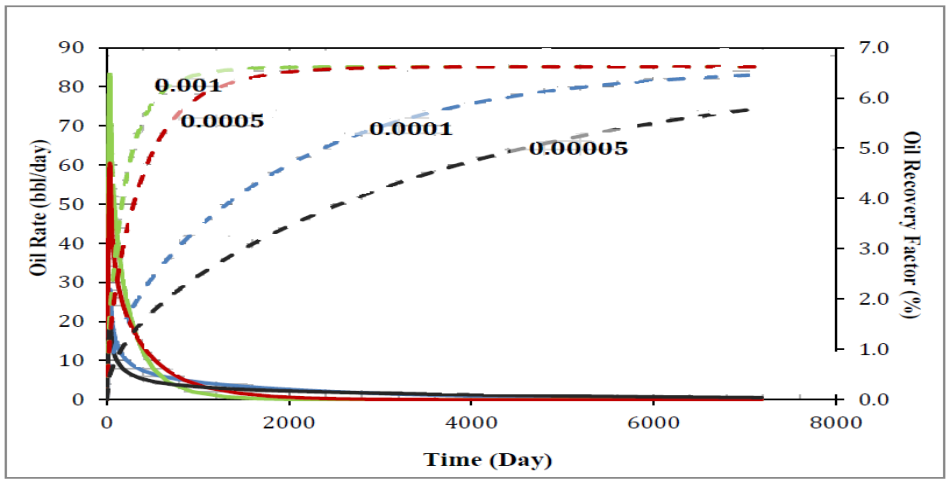

Figure 4.12 Oil Rate and Oil Recovery Factor vs. Time (Matrix Permeability Sensitivity)

4. Conclusion

This thesis basically considered the modeling of fluid recovery from shale reservoir systems. Shale oil reservoirs were considered in this study with Eagle Ford as a case study. The methodology basically involved the development of a mathematical model that incorporates the basic development strategies and the simulation of this model to determine the applicability of the model and how reservoir and operational conditions and parameters affect fluid recovery from these unconventional reservoirs.

As shale resources become a focus of exploration and production activity in North America, oil and gas industry made tremendous efforts to research on stimulating the oil and gas production from shale reservoirs. The horizontal well with multiple transverse fractures has proven to be an effective strategy for shale gas reservoir exploitation and it is also used in producing shale oil by some oil companies. However, due to complex conditions of shale oil, the production performance is still not attractive. Improving oil recovery will be a great challenge in the development of shale oil reservoirs. Thus, we initiate our work, considering conventional EOR techniques, gas and water injection, which has been successfully, implemented in conventional and some unconventional tight oil reservoirs for a long time, to assess the potential of improving shale oil recovery by EOR techniques.

The cases chosen for this study are not comprehensive, but may represent somewhat typical situations. A black-oil simulator ECLIPSE (E-300, Office 2015.1) was used in this study to simulate a number of production plans for gas flooding and water flooding. 8470 (22 x 55 x 7) grid-cells are used to build a 200ft long×1000ft wide×200ft thick reservoir model. In this model we use 1-ft wide cells with 41.65 md-ft conductivity which was located at the boundary of the model to simulate the physical flow between two hydraulic fractures. Three typical production plans for gas and water injection were presented in this thesis respectively. In spite of the limited work of this study, it is still possible to reach some conclusions.

- Because of the ultra-low permeability of shale reservoirs, in a 200 ft wide shale oil reservoir model, it's more difficult for injection materials transmit and displace oil than that in conventional reservoirs or tight oil reservoirs which have better condition than shale reservoirs. Although in miscible condition, oil viscosity just can be reduced around the fracture, the main effect of gas injection is pressure maintenance.
- According to sensitivity analysis, matrix permeability is the main parameter causing low oil recovery from shale reservoirs. Designing closer fracture spacing will have an obviously positive influence on shale oil production. It, not only leads a higher initial production rate but also a much better sweep efficiency for miscible gas flooding, resulting an attractive ultimate oil recovery factor.

4.1. Recommendations

- Gas flooding in two horizontal wells with multiple transverse hydraulic fracture should be tested.
- Water injection in shale oil reservoir was not considered because of the inherent assumption that water injection has no potential in the development of shale oil reservoirs absolutely. Future studies should account for water injection effect in reservoir.
- Economic analysis should be done in the future work for the determination of the optimum injection, production and completion plan.

5. References

AER. (2016). *Energy Outlook Around The Globe.* Texas: Annual Energy Report - https://www.annualenergyreport/commmon_wealth_usa/ghykljjiubvvvhvhbjijnn.

Alfonso, R. (2016). *Improving Recovery of Liquids from Shales Through Gas Injection.* Calgary, Alberta: Prataz Clazo Press.

Amy, F. (2015). *Compositional Simulation Of CO2 Enhanced Oil Recovery In Unconventional Liquid Reservoirs.* Texas: A & M University.

Babadagli, T. (2001). Scalling of Concurrent apilary of Imbibition for surfactant and Polymer Injection in Naturally Fratured Reservoirs. *SPE Jornal Dec*, 465-478.

Chen, K. (2013). *Evaluation of Eor Potential by Gas and Water Flooding in Shale Oil Reservoirs.* Texas: Texas Tech University.

Dusseault, M. (2002). *Cold Heavey Oil Production with Sand In The Canadian Heavy Oil Industry.* Quebec: Caritson Publishing.

Geraldine, G. (2005). *Enhanced Oil Recovery: An Alterntive Method For Improving Shale Gas Recovery.* Chicago: Mulfin Publishing: The Face.

Javadpour, F. (2009). Nanopores and Apparent Permeability of Gas Flow in Mudrocks (Shales and Siltstone). *Journal of Canadian Petroleum Tech*(48), 16-21.

Phillips, Z., Herverson, R., Strauss, S., Layman II, J., & Green, T. (2007). A case study in the bakken formation: changes to hydraulic fracture stimulation treatments resultsin improved oil production and Reduced Treatment Costs. . *Paper SPE 108045 Presented by Rocky Mountian Oil and Gas Technology Symposium*, 16-18.

Rahman, M., Aghighi, M., Rahman, S., & Ravoof, S. (2009). Interaction Between Induced Hydraulic Fracture and Pre-Existing Natural Fracture in a Poro-Elastic Environment: Effect of Pore Pressure Change and the Orientation of Natural Fractures. *Asia Pacific Oil and Gas Conference & Exhibition* (pp. 234-245). Migwork Press.

Roger, S. (2017). *Shale Discovery Around The World: The Coming Boom.* Mumbai: Journal of Petroleum Technology.

Schlumberger. (2016). *Characterization of Shale formations: An overview of the Eagle Ford.* Chicago: Schlumberger Company Limited.

Sheng, J. (2013). Comparison of the Effect of Wettability Alteration and IFT Reduction on Oil Recorvery in Carbonate Reservoirs. *Asia Pecific J. Chem. Eng. 8 (1)*, 154-161.

Sheng, J. (2013). Introduction to MEOR ans its Field Application in China. *Enhanced oil recorvery in field cases*, 54-69.

Sheng, J. (2013). Surfactant Enhanced Oil Recorvery in Carbonate Reservoir. *Ehanced Oil Recorvery Cases*, 60-65.

Tao Wan, B. (2013). *Evaluation of the EOR Potential in Shale Oil Reservoirs by Cyclic Gas Injection.* HOUSTON, TEXAS: Texas Tech University.

Terry, R. (2001). Ehanced Oil Recorvery . *Enclopedia of Physical Science and Technology, Third Edition, 18*, 503-518.

Wang, D., Butler, R., Liu, H., & Ahmed, S. (2011). Flow Rate Behaviour and Imbibition in Shale. *SPE*, 458-492.